STATE RESEARCH CENTER OF RUSSIA
INSTITUTE FOR HIGH ENERGY PHYSICS

IHEP 2010–1

S.P. Denisov, V.N. Evdokimov, A.V. Kozelov, N.N. Prokopenko,
M.M. Soldatov, D.A. Stoyanova, V.I. Yakimchuk

CHERENKOV COUNTER FOR BUNCH INTENSITY MEASUREMENT

Protvino 2010

UDK 539.1.074 M-24

Abstract

Denisov S.P. et al. Cherenkov Counter for Bunch Intensity Measurement: IHEP Preprint 2010-1. – Protvino, 2010. – p. 12, figs. 10, tables 3, refs.: 6.

Cherenkov counter for bunch intensity measurements in slow extracted beams from the IHEP accelerator is described. The dynamic range is from 1 to 10^6 particles/bunch and bunch frequency is up to 6×10^6/s. Cherenkov light is detected by XP 2020 PMT. XP 2020 signal pulse height and delay were measured as a function of XP 2020 high voltage from 0.8 to 2.7 kV using green and blue LED's. Results of the counter calibration in the 50 GeV proton beam are presented. The model used to fit the counter height pulse spectra is discussed.

Аннотация

Денисов С.П. и др. Черенковский счётчик для измерения интенсивности банчей: Препринт ИФВЭ 2010-1. – Протвино, 2010. – 12 с., 10 рис., 3 табл., библиогр.: 6.

Описан черенковский счётчик для измерения числа протонов в банчах, выведенных из ускорителя ИФВЭ при помощи системы медленного вывода. Диапазон измерений – от 1 до 10^6 частиц/банч и максимальная частота банчей – 6×10^6/сек. Черенковский свет регистрируется при помощи ФЭУ XP2020. Приведены результаты измерений амплитуды сигнала с ФЭУ XP2020 и задержки в зависимости от высокого напряжения на нём (в диапазоне от 0.8 до 2.7 кВ) с использованием зеленого и голубого светодиодов. Представлены результаты калибровки счётчика на 50 ГэВ протонном пучке. Рассмотрена модель для описания амплитудных спектров сигналов со счётчика.

Introduction

This work was done in the frame of the experiment on studies of modules of the endcap and forward liquid argon calorimeters of ATLAS facility at LHC in the high intensity 50 GeV proton beam extracted from the IHEP accelerator to the beam channel №23 using a bent crystal. The beam used in the experiment consists of 30 ns bunches separated by 1 μs intervals. The spill length is 1s and the accelerator cycle is equal to 10 s. The beam intensity is changed from 10^6 to 10^{12} ppp. Thus the train of 10^6 bunches passes through the setup each 10 s and the average number of protons per bunch varies from 1 to 10^6. At the highest intensity the particle flux through the forward calorimeter module corresponds to those expected at SLHC. The minimal interval between bunches in the IHEP accelerator is 165 ns and maximal number of bunches per second is equal to $6 \cdot 10^6$.

Initially the beam intensity in the channel №23 was measured by the secondary emission chamber SEC (in the range 10^{10}–10^{12} s^{-1}), ionization chamber IC (at 10^7–10^{11} s^{-1}), and scintillation counters and hodoscopes (at intensity less than 10^7 c^{-1}). SEC and IC are capable to measure a proton flux integrated over the beam spill. In addition, special calibration procedure [1] based on simultaneous irradiation of these detectors and Al foil with 10^{14} protons followed by the measurement of the foil activation is necessary. The typical calibration error is about 20%.

At the beginning of the experiment it was assumed that protons are uniformly distributed between bunches in the given spill. But it turned out that this is not the case: the number of particles per bunch in the same spill can differ by a factor of 2-3. Besides the calorimeter signal from a given bunch depends on the intensity of previous bunches due to

low drift velocity of Ar ions. That is why a detector capable to measure the intensity of each bunch became highly desirable. It would be also important if this detector could measure the absolute bunch intensity in the whole interval from 1 to 10^6 without calibration with aluminum foil.

Counter design and simulation

Such a detector based on registration of cherenkov light emitted by protons in air or freon CF_4 has been designed and produced at IHEP. Its design is shown in Fig. 1. For 50 GeV protons at 20° C and 760 Torr the threshold pressure and angle of cherenkov emission are equal to 0.4 atm and 23.4 mrad for freon and 0.4 atm and 14.1 mrad for air. The cherenkov light reflected by thin (100 μm) aluminized mylar mirror inclined at 45° in respect to the beam direction collected onto XP 2020 PMT (Fig. 1). To improve light collection an aluminized mylar conical mirror is installed in front of the PMT. In the wavelength range from 0.270 μm to 0.640 μm corresponding to a full width of the XP 2020 spectral characteristic [2] the mean numbers of radiated photons are 25.6 and 9.3 for freon and air at 1 atm.

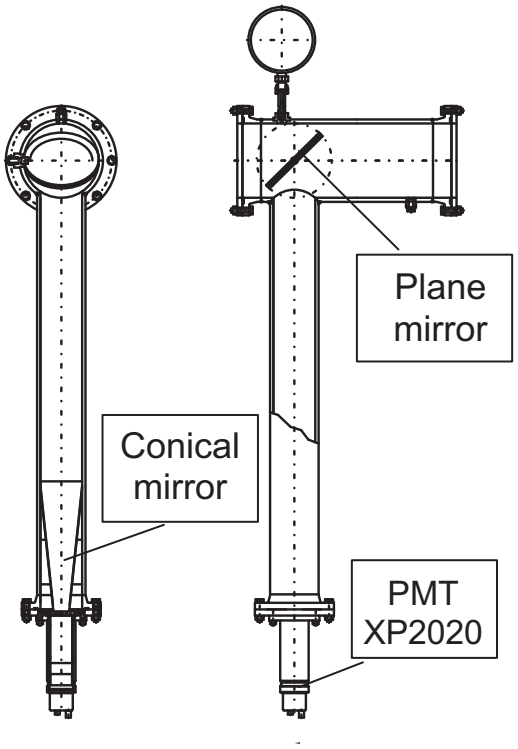

Fig. 1. Design of the Cherenkov counter.

The light collection was simulated by Monte Carlo using 0.6 reflection coefficient for both mirrors and Gaussian radial (σ=5 mm) and angular (σ=5 mrad) distributions of beam particles. It was found that 53% and 41% of emitted photons reach the PMT for air and freon respectively. Better light collection for air is due to smaller radiation angle. In the case of air almost all photons reach the PMT missing the conical mirror while for freon considerable part of photons is reflected by this mirror. The results weakly depend on beam transversal and angular distributions. For example increase of σ's by factor of 2 changes the light collection efficiency by 10% for air and less than 1% for freon. Assuming 0.1 quantum yield for the XP 2020 and 100% probability of single photoelectron registration the efficiency of the counter to detect a 50 GeV proton is estimated to be 0.39 (air) and 0.65 (freon) at 1 atm. gas pressure. The uncertainty of these values is about 20%.

Counter calibration

It is rather difficult to cover the whole range of cherenkov counter amplitudes *A* with fixed values of working gas pressure *P* and PMT high voltage *HV*. Therefore *A(P)* and *A(HV)* dependencies should be measured. The test setup for *A(HV)* measurement is shown in Fig. 2. Generator BNC 8010 fired 2 LEDs emitting blue and green light. The light passed through an optical fiber to XP 2020 photocathode. The pulse heights of PMT signals were measured by a digital scope with 5% uncertainty.

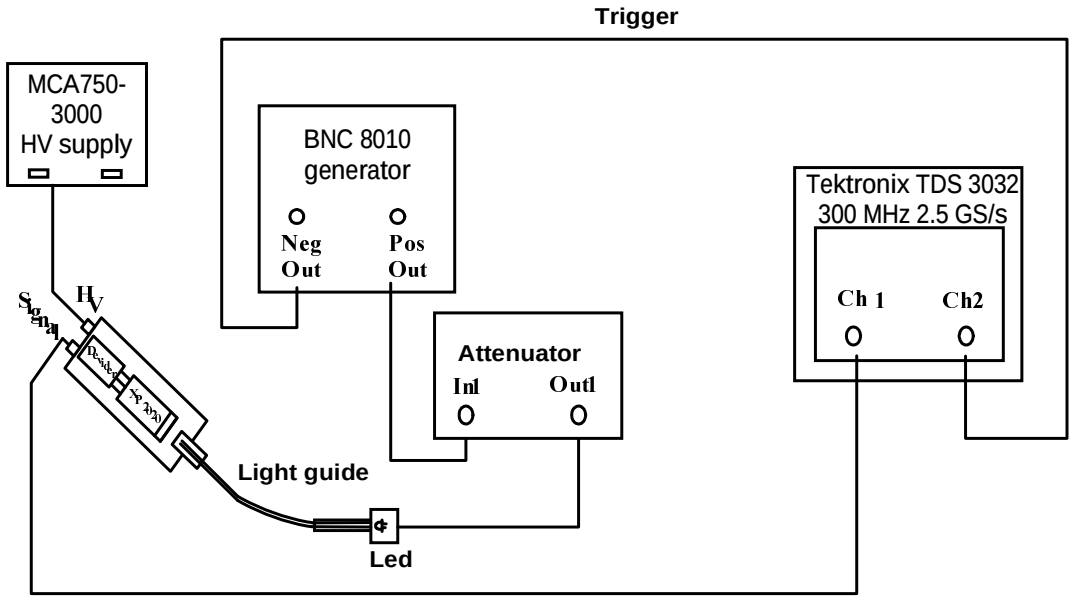

Fig. 2. Test setup for *A(HV)* measurements.

A(HV) dependencies measured for two PMTs are presented in Fig.3. They follow a power law in the whole studied HV range where the signal pulse height is changed by 5 orders of magnitude (see also [3]). Power exponents are close to 10 and weakly depend on the light wavelength (Table 1).

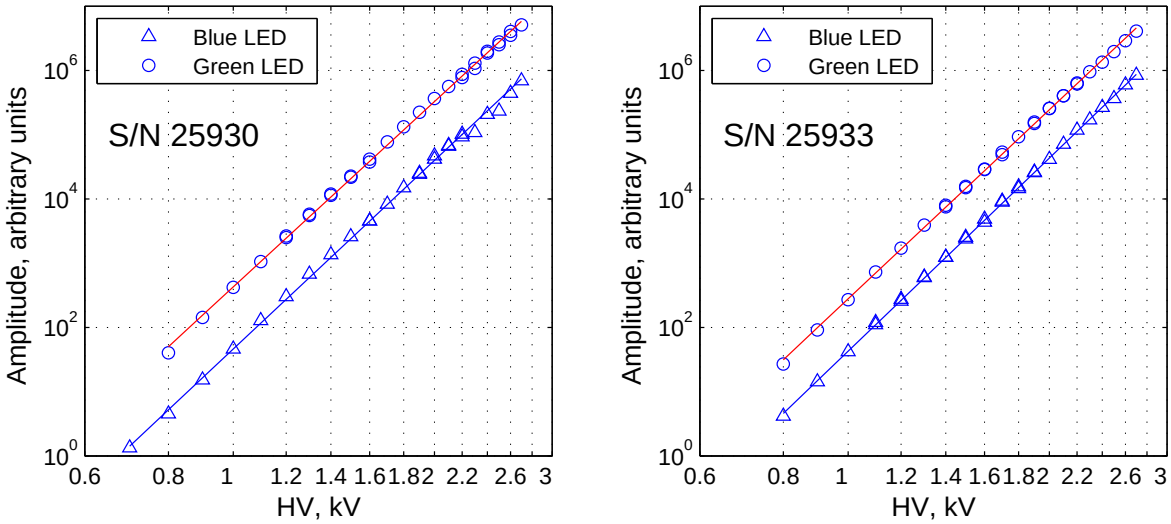

Fig. 3. PMT signal pulse height vs HV for two XP 2020. Values of pulse heights obtained with the green LED are increased by factor of 10 for better visualization.

Table 1. Power exponents of *A(HV)* dependence .

PMT *S/N*	25930	25933
Blue LED	9.75±0.03	9.99±0.03
Green LED	9.59±0.03	9.78±0.03
Beam measurements	9.82±0.02	9.84±0.03

To obtain an absolute scale for the counter amplitude in units of the average signal from a single proton the special experiment was performed at beam channel №2B of the IHEP accelerator (Fig. 4). Slow extracted debunched 50 GeV proton beam with intensity of ~$5\cdot10^4$ s^{-1} passed through three trigger scintillation counters and Cherenkov counter. The size of S1 and S2 counters was 2×2 $см^2$. They formed a beam with parameters (size and divergence) similar to those in the channel №23. S2 counter with diameter of 12 cm was used to monitor full beam intensity. TC/T ratio was used to estimate Cherenkov counter efficiency, where T=S1·S2·S3 is a trigger signal and TC is a coincidence of T with a signal from Cherenkov counter. The spill uniformity was controlled with “intensimeter” [4].

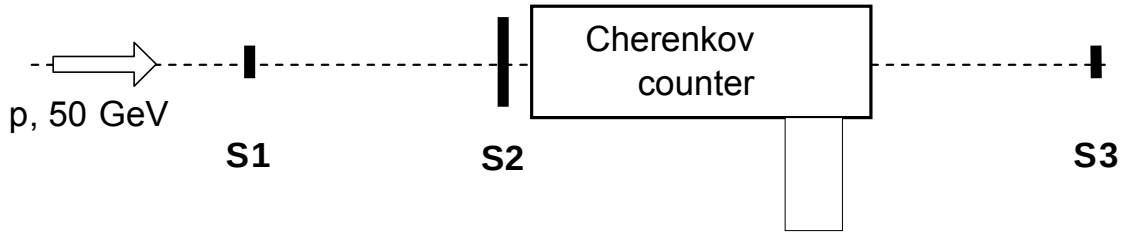

Fig. 4. Experimental setup.

Signals from the Cherenkov counter were fed to a LeCroy 2249a ADC gated with 50 ns T signal. The probability that 2 protons passed through the counter within the gate was less than 1%. The experiment consisted in measuring the Cherenkov counter efficiency and its pulse height spectra at different values of pressure and high voltage. About 50000 events were collected for each *P* and *HV*.

Beam calibration results

The dependencies of counter efficiency on high voltage for different air pressures are shown in Fig. 5. They reach a plateau at *HV* >2.3 kV. This means that the efficiency of a single photoelectron registration becomes close to 1. Threshold curves for one of the PMTs are shown in Fig. 6. At *HV* >2.3 kV they can be parametrized as

$$\varepsilon(P) = \begin{cases} 1-\exp(-a\cdot(P-P_0)), & P \geq P_0 \\ 0 & P < P_0 \end{cases},$$

where P_0 is a threshold pressure and $\mu = a\cdot(P - P_0)$ is an average number of photoelectrons. Results of the fits are shown in Table 2. From the Table it follows that efficiencies of the counter at atmospheric pressure of freon and air are close to those obtained in simulations.

Table 2. Fit parameters obtained at HV=2.6 kV.

PMT *S/N*	Gas	*a*	P_0 *(atm)*	ε (at 1 *atm*)
25930	Air	1.19±0.05	0.666±0.003	0.33±0.02
	CF_4	1.86±0.03	0.392±0.003	0.68±0.02
25933	Air	1.11± 0.04	0.668±0.003	0.31±0.02
	CF4	1.72±0.03	0.390±0.003	0.65±0.02

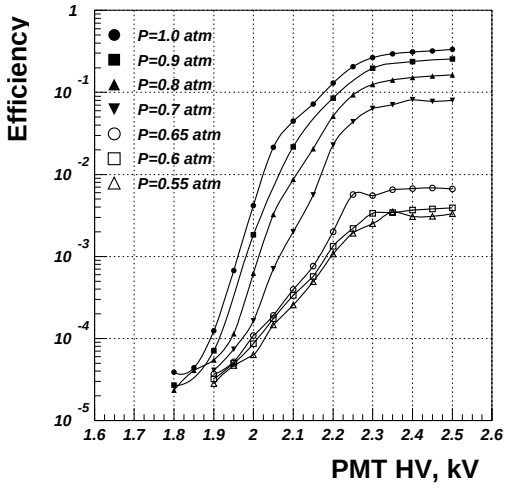

Fig. 5. Counter efficiency vs PMT high voltage.

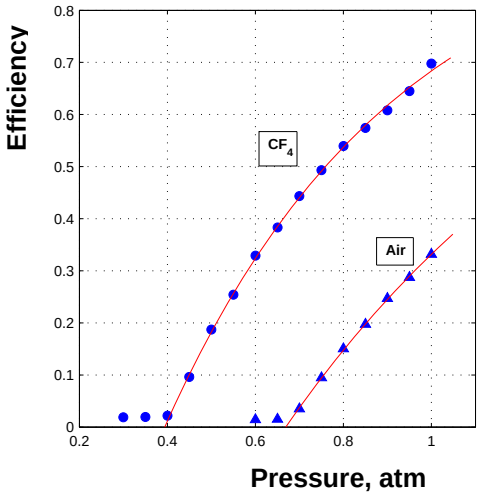

Fig. 6. Counter efficiency vs freon and air pressures at HV=2.6 кВ.

Pulse height spectra of Cherenkov counter signals are shown in Fig. 7. The following model [5] was used to describe these spectra. A single photoelectron spectrum was represented as a sum of exponential and Gaussian distributions:

$$\tilde{S}_1(x) = \begin{cases} w\cdot\lambda\cdot e^{-\lambda x} + \dfrac{1-w}{\sqrt{2\pi}\sigma_1}\exp\left(-\dfrac{(x-x_1)^2}{2\sigma_1^2}\right) = w\cdot E(x) + (1-w)\cdot G(x-x_1,\sigma_1^2), & x \ge 0 \\ 0, & x < 0 \end{cases}, \quad (1)$$

where λ , x_1 and σ_1 are the parameters of the exponential and Gaussian distribution and w is the fraction of events in the exponential part. Neglecting the Gaussian tail at x<0 one can calculate the mean value Q_1 and variance σ^2 of a single photoelectron spectra:

$$Q_1 \approx \frac{w}{\lambda} + (1-w)\cdot x_1, \quad \sigma^2 \approx (1-w)(\sigma_1^2 + Q_1^2) + 2\frac{w}{\lambda} - Q_1^2 \quad (2)$$

Pulse height distribution for n photoelectrons can be obtained as n-fold convolution of the single photoelectron spectra:

$$\tilde{S}_n = \underbrace{\tilde{S}_1 \otimes \tilde{S}_1 \otimes \ldots \otimes \tilde{S}_1}_{n} = (w\cdot E + (1-w)\cdot G)^{(n)}, \quad (3)$$

where $f(x)\otimes g(x) = \int_{-\infty}^{\infty} f(y)\cdot g(x-y)dy$.

To describe the experimental data one should also take into account the ADC pedestal distribution S_{PED} that has a Gaussian shape: $S_{PED} = G(x-Q_0,\sigma_0^2)$. Thus n photoelectron

spectrum can be written as

$$S_n = \tilde{S}_n \otimes S_{PED}\,. \tag{4}$$

From (1), (3) and (4) one can obtain:

$$S_n = (w\cdot E + (1-w)\cdot G)^{(n)} \otimes S_{PED} = \sum_{k=0}^{n} \binom{n}{k} \cdot w^{n-k} \cdot (1-w)^k \cdot E_{n-k} \otimes G_k$$

$$E_k(x) = \begin{cases} \delta(x), & k = 0 \\ \dfrac{1}{(k-1)!}\lambda^k x^{k-1} e^{-\lambda x}, & k \geq 1 \end{cases}$$

$$G_k(x) = G(x - Q_0 - k\cdot x_1, \sigma_0^2 + k\cdot\sigma_1^2) \tag{5}$$

where $\delta(x)$ is the Dirac function, and $\binom{n}{k}$ are the binomial coefficients.

All convolutions in (5) can be evaluated analytically using the relation

$$\int_0^\infty x^{v-1} e^{-\beta x^2 - \gamma x} = (2\beta)^{-\frac{v}{2}} \cdot \exp\left(-\frac{\gamma^2}{8\beta}\right) \cdot D_{-v}\left(\frac{\gamma}{\sqrt{2\beta}}\right),$$

where D is the parabolic cylinder function [6]. For large number of photoelectrons ($n>3$) it is more convenient to use the following approximation

$$S_n(x) \approx G(x - Q_0 - n\cdot Q_1, \sigma_0^2 + n\cdot\sigma^2), \quad n > 3, \tag{6}$$

where Q_1 and σ are defined in (2). The formulas for S_n at $n=2,3$ are given in the Appendix.

Since the probability of overlapping of signals from two particles is negligable (see above) the photoelectron distribution follows a Poisson law, and finally pulse height spectra of signals from the Cherenkov counter is described by

$$S(x) = N\cdot\sum_{n=0}^{\infty} P(n,\mu)\cdot S_n(x) = N\cdot\sum_{n=0}^{\infty} \frac{\mu^n e^{-\mu}}{n!}\cdot S_n(x), \tag{7}$$

where N is the number of events, and μ is an average number of photoelectrons per 50 GeV proton.

Two Cherenkov counter spectra fitted with (7) are shown in Fig.8. Fit parameters are: Q_0 and σ_0 are the mean and standard deviation of ADC pedestal, Q_1 is the mean of a single photoelectron spectrum $\tilde{S}_1(x)$; σ_1, w and λ are the parameters of $\tilde{S}_1(x)$ from equation (1), μ is an average number of photoelectrons. Parameter x_1 was calculated from (2).

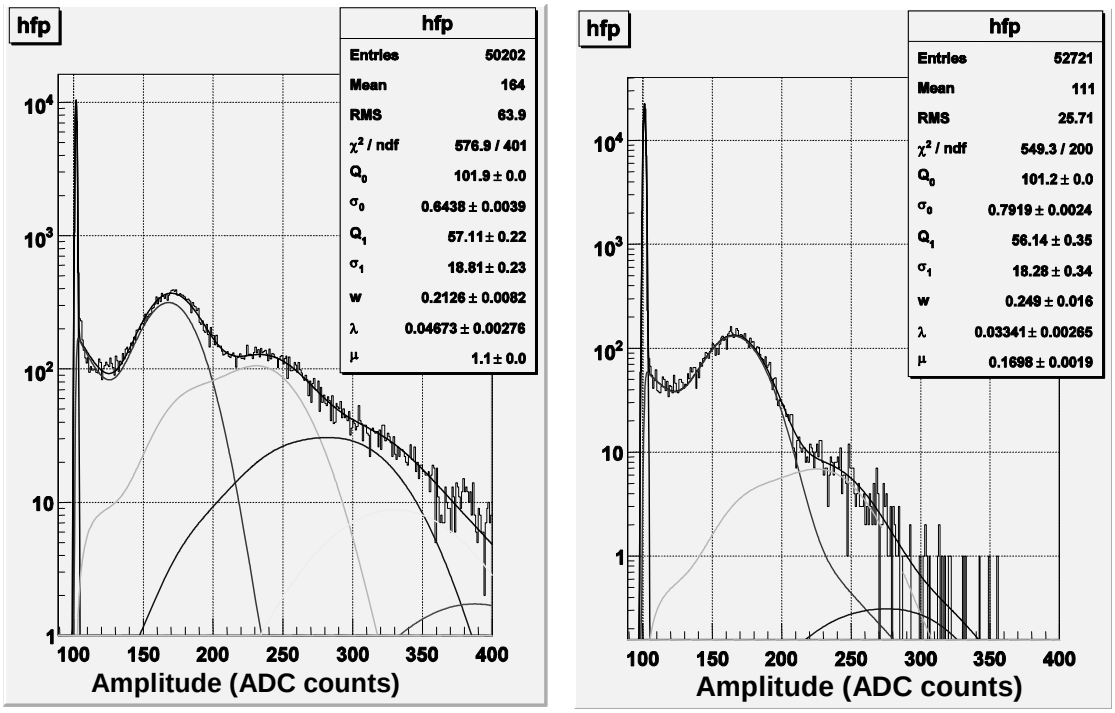

Fig. 7. Cherenkov counter pulse height spectra measured at HV= 2.6 kV and at 0.95 atm freon pressure (right) and at 0.8 atm. air pressure. Histograms present the experimental data and lines show the results of the fit and contributions from one, two, three and four photoelectrons.

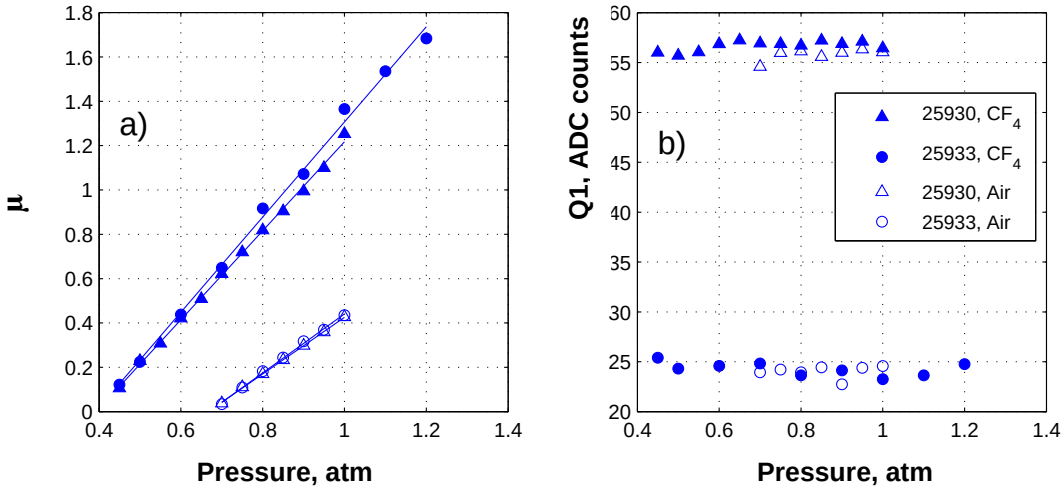

Fig. 8. Average number of photoelectrons (a) and mean amplitude of a single photoelectron spectrum (b) vs pressure in the Cherenkov counter at HV= 2.6 kV.

Values of μ and Q_1 obtained from the fit are shown in Fig.8 as a function of pressure in the Cherenkov counter. As expected the average number of photoelectrons linearly depends on pressure. Parameters of this dependence were used to calculate threshold pressures (see Table 3) which turns out to be in good agreement with the values obtained from threshold

curves (see Table 2). The mean of the single photoelectron spectra do not depend on pressure and gas type and is determined only by the PMT gain.

Table 3. Threshold pressures.

PMT *S/N*	Gas	P_0 from $\mu(P)$
25930	Air	0.658±0.002
	CF_4	0.392±0.002
25933	Air	0.668±0.002
	CF_4	0.391±0.002

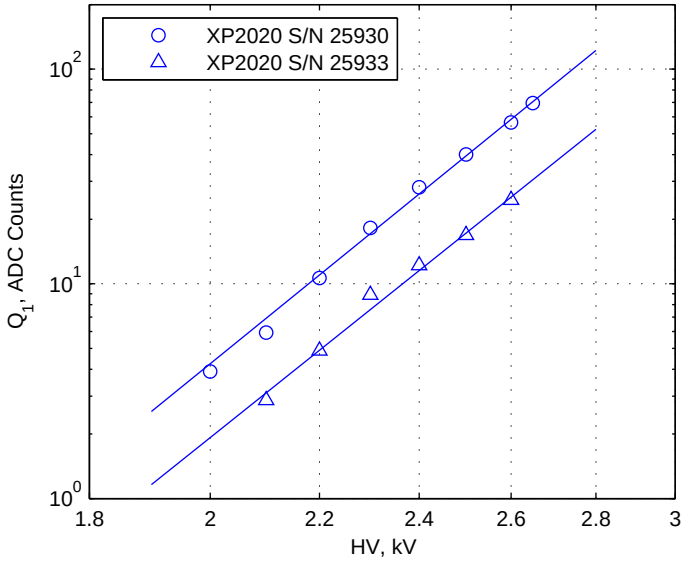

Fig. 9. Mean amplitude of a single photoelectron spectrum as a function of high voltage the at air pressure of 1 atm.

Dependencies of Q_1 on high voltage for two PMTs are shown in Fig. 9. They follow a power law. The values of power exponents are shown in the last row of Table 1. They are in a good agreement with LED measurements. Mean values of the Cherenkov counter spectra agree with $\mu \cdot Q_1$ within 1-2%.

Calibration data obtained with LED's and in the proton beam allows one to calculate the mean amplitude for a single proton in wide ranges of PMT high voltage and gas pressure in the Cherenkov counter which can be used to estimate the number of protons in the bunch up to 10^6.

Results of measurements at the beam channel №23

The Cherenkov counter was used for bunch intensity measurements in the November 2008 run. A 50 GeV/c proton beam was extracted from the accelerator to the channel №23. A custom 6 MHz ADC was used in the experiment. It has the following characteristics: 12 bit dynamic range, 650 pC maximum measured charge, integral nonlinearity is less than 0.1%, 70 ns internal gate width, 32 Mbytes memory. the ADC has inputs for the event tag signal and 6MHz RF from the accelerator which is used to form the ADC gate synchronized with the beam bunches. Distribution of bunch intensities in one of the spills is shown in Fig. 10. From this figure it follows that the number of particles per bunch can vary by an order of magnitude.

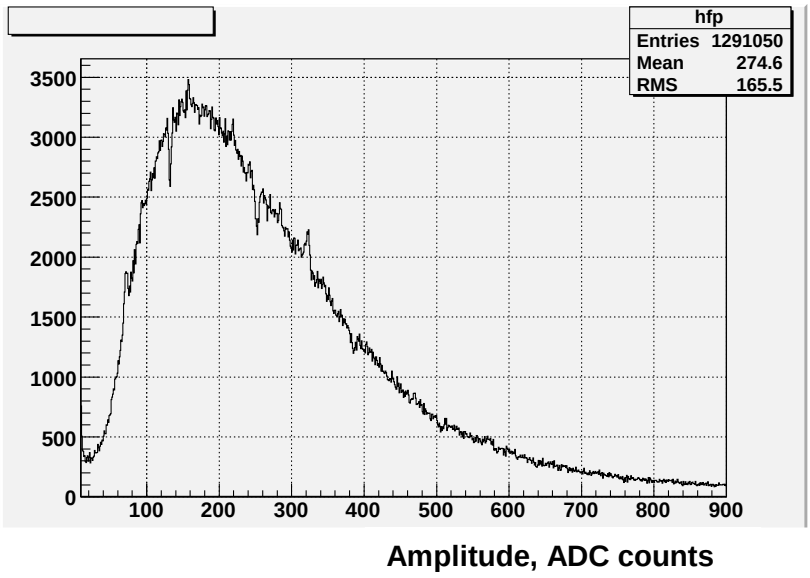

Fig. 10. Bunch intensity distribution in one of the spills measured at the average beam intensity of $3 \cdot 10^8$ protons/s in the channel #23 (HV=2.1 kV, P=1 atm. of air).

Comparison of intensity measurements with the Cherenkov counter and the ionization chamber IC in the range of 10^8-10^{11} protons/s shows that IC gives 20-30% higher values than the Cherenkov counter. This difference is within the uncertainty of IC calibration.

Conclusion

A simple Cherenkov counter for bunch intensity measurements was designed, produced and tested at the IHEP accelerator. It allows one to measure the number of protons in each bunch of $6 \cdot 10^6$ per second. Statistical error depends on the number of photoelectrons

and the systematic one is equal to 5%. The last value is mainly due to uncertainty in calibration and can be easily reduced to 2-3%.

Acknowledgements

We appreciate the support of A.V. Levin, V.I. Suzdalev, I.N. Belaykov, N.M. Belyakov, P.I. Galukh, S.A. Zvyagintsev, V.V. Konstantinov, O.N. Romashev and I.V. Shvabovich in design, construction and tests of the Cherenkov counter. This study was supported in part by the Russian Fund for Basic Research (grant 09-02-00303-a).

References

[1] J.B. Cumming, J. Hudis, A.M. Poskanzer et al. Phys. Rev. 128, 2392-2397 (1962); G.I. Krupny, D.V. Snitko, A.A.Yanovich. Cross-Section of Responses Al^{27}(p,spall)Be^{7}, Al^{27}(p, 3p3n)Na^{22} and Al^{27}(p, 3pn)Na^{24} in a Range of Energies of Protons 37 MeV - 70 GeV. // Atomic Energy, v. 89, №.5, 939-941 (2000).

[2] http://www.photonis.com/upload/industryscience/pdf/pmt/XP2020.pdf

[3] S.O. Flyckt, C. Marmonier. // Photomultiplier tubes principles & applications. – Photonis, 2002.

[4] A.V.Kozelov, A.A.Lebedev, S.A.Medved, Yu.V.Mikhailov. Time resolved measurement of an output beam's intensity. // Instrum. Exp. Tech. 37, 160-162 (1994).

[5] R. Dossi, A. Ianni, G. Ranucci, O.Y. Smirnov, Methods for precise photoelectron counting with photomultipliers. // Nucl. Instrum. Meth. A **451**, 623 (2000).

[6] I.S. Gradshtein, I.M. Ryzhik, Tables of integrals, sums, rows and products. – Moscow, 1963.

Appendix

The distribution of signal pulse heghts for two or three photoelectrons can be analytically expressed as a combination of exponents and error function $erf(x) = \frac{2}{\sqrt{\pi}} \int_0^x \exp(-y^2) dy$:

$$S_2(x) = w^2 E_2 \otimes G_0 + 2w(1-w) E_1 \otimes G_1 + (1-w)^2 G_2 ,$$

where

$$E_2 \otimes G_0 = \lambda^2 \frac{\sigma_0}{\sqrt{2\pi}} \exp\left(-\frac{(x-Q_0)^2}{2\sigma_0^2}\right) +$$
$$+\frac{\lambda^2}{2}\left(1+erf\left(\frac{x-Q_0-\lambda\sigma_0^2}{\sqrt{2}\cdot\sigma_0}\right)\right)\cdot(x-Q_0-\lambda\sigma_0^2)\cdot\exp\left(-\lambda(x-Q_0-\tfrac{1}{2}\lambda\sigma_0^2)\right)$$

$$E_1 \otimes G_1 = \frac{\lambda}{2}\exp\left(-\lambda\left(x-Q_0-Q_1-\frac{\lambda}{2}(\sigma_0^2+\sigma_1^2)\right)\right)\cdot\left(1+erf\left(\frac{x-Q_0-Q_1-\lambda(\sigma_0^2+\sigma_1^2)}{\sqrt{2(\sigma_0^2+\sigma_1^2)}}\right)\right)$$

$$G_2 = \frac{1}{\sqrt{2\pi(\sigma_0^2+2\sigma_1^2)}}\cdot\exp\left(-\frac{(x-Q_0-2Q_1)^2}{2(\sigma_0^2+2\sigma_1^2)}\right).$$

$$S_3(x) = w^3 E_3 \otimes G_0 + 3w^2(1-w)E_2 \otimes G_1 + 3w(1-w)^3 E_1 \otimes G_2 + (1-w)^3 G_3,$$

where

$$E_3 \otimes G_0 = \lambda^3 \frac{(x-Q_0)\sigma_0 - \lambda\sigma_0^3}{2\sqrt{2\pi}} \exp\left(-\frac{(x-Q_0)^2}{2\sigma_0^2}\right) +$$
$$+\frac{\lambda^3}{4}\left(1+erf\left(\frac{x-Q_0-\lambda\sigma_0^2}{\sqrt{2}\cdot\sigma_0}\right)\right)\cdot\left((x-Q_0-\lambda\sigma_0^2)^2+\sigma_0^2\right)\cdot\exp\left(-\lambda(x-Q_0-\tfrac{1}{2}\lambda\sigma_0^2)\right)$$

$$E_2 \otimes G_1 = \lambda^2\sqrt{\frac{\sigma_0^2+\sigma_1^2}{2\pi}}\exp\left(-\frac{(x-Q_0-Q_1)^2}{2(\sigma_0^2+\sigma_1^2)}\right) +$$
$$+\frac{\lambda^2}{2}\left(1+erf\left(\frac{x-Q_0-Q_1-\lambda(\sigma_0^2+\sigma_1^2)}{\sqrt{2(\sigma_0^2+\sigma_1^2)}}\right)\right)\cdot(x-Q_0-Q_1-\lambda(\sigma_0^2+\sigma_1^2))\cdot\exp\left(-\lambda(x-Q_0-Q_1-\tfrac{1}{2}\lambda(\sigma_0^2+\sigma_1^2))\right)$$

$$E_1 \otimes G_2 = \frac{\lambda}{2}\exp\left(-\lambda\left(x-Q_0-2Q_1-\frac{\lambda}{2}(\sigma_0^2+2\sigma_1^2)\right)\right)\cdot\left(1+erf\left(\frac{x-Q_0-2Q_1-\lambda(\sigma_0^2+2\sigma_1^2)}{\sqrt{2(\sigma_0^2+2\sigma_1^2)}}\right)\right)$$

$$G_3 = \frac{1}{\sqrt{2\pi(\sigma_0^2+3\sigma_1^2)}}\cdot\exp\left(-\frac{(x-Q_0-3Q_1)^2}{2(\sigma_0^2+3\sigma_1^2)}\right)$$

Received March 1, 2010.

С.П. Денисов и др.
Черенковский счётчик для измерения интенсивности банчей.

Оригинал-макет подготовлен авторами.

Подписано к печати 01.03.2010. Формат 60 × 84/16. Офсетная печать.
Печ. л. 0,875. Уч.- изд. л. 1,344. Тираж 100. Заказ 15. Индекс 3649.

ГНЦ РФ Институт физики высоких энергий,
142281, Протвино Московской обл.

Индекс 3649

П Р Е П Р И Н Т 2010-1, ИФВЭ, 2010